Formation of graphene and hexagonal boron nitride on Rh(111) studied by in-situ scanning tunneling microscopy

Dong, G.

Chapter 3 Introduction of part I

3.1 Background

On the Rh(111) surface, hexagonal boron nitride (*h*-BN) adopts a highly regular superstructure, with 2 nm diameter depressions and a 3.2 nm period. Similar structures are found on other metal surfaces. This so-called *nanomesh* [6] serves as a two-dimensional scaffold for deposition of bucky balls and other, functional molecules [6, 18], which may lead to interesting e.g. electronic, magnetic**,** or catalytic properties and applications. The nanomesh coating has been demonstrated to remain intact under ambient conditions [12], in liquids [19], and at high temperatures [6], thus protecting the underlying metal. The combination of *h*-BN and graphene provides opportunities for sophisticated band gap engineering in the graphene [75-77] and for advanced device development [78]. The atomic structure of the nanomesh has been unraveled, by a combination of Scanning Tunneling Microscopy (STM) [6, 14], surface X-ray diffraction (SXRD) [12], and theoretical calculations [10, 11]. It is a single, highly corrugated layer of *h*-BN, with 13 × 13 unit cells of the *h*-BN lattice fitting onto 12 × 12 unit cells of the underlying Rh(111) surface.

In view of the large super-cell, containing 338 overlayer atoms, the superb quality of the observed nanomesh patterns is quite surprising. The procedure, originally introduced by Corso *et al.* for the deposition of a nanomesh film, is to expose the Rh(111) surface to borazine $(HBNH)_3$ gas at 1050 K [6]. What is the role of this high temperature? It could be that a high temperature is necessary to crack the borazine molecules, releasing hydrogen, and possibly rupturing B-N bonds, in order to form reactive precursors, which stick sufficiently strongly to the surface and serve as the growth units, from which the overlayer can be assembled. One can also imagine that a high temperature would be required to provide sufficient lateral mobility for crystallizing the otherwise disordered

overlayer into the perfectly periodic nanomesh structure. While the high temperature serves as an important clue, it also poses a significant experimental difficulty.

3.2 Experimental methods

All measurements were carried out under ultrahigh vacuum (UHV), with a variable-temperature STM setup, which allowed fast scanning and imaging over a wide range of temperatures and during substantial temperature changes [33, 34]. The base pressure of the system was 1.5×10^{-11} mbar. All pressures, including that of the borazine gas, were measured with an ion gauge, without considering the differences in the sensitivities for the different gases. Sample temperatures were measured by a K-type thermocouple, spot-welded directly onto the Rh single crystal. The crystal was heated from the rear side by a filament, using either by thermal radiation or by electron bombardment, extracting electrons from the filament and accelerating them through a voltage of -600 V between the filament and the sample. This allowed the sample to be heated from room temperature to 1300 K in 10 seconds. The Rh sample was cleaned by cycles of Ar^+ ion sputtering, followed by flash annealing to 1300 K, and exposure of the sample to 2 to 3 $\times10^{-7}$ mbar of O_2 for 1 to 2 hours, at temperatures of 700-800 K. The latter step proved necessary for removal of carbon surface contamination, which segregated out of the bulk. Residual O was removed from the Rh surface by flashing the sample to 1000 K [73]. After having repeated this cycle at least 10 times, no C contamination could be detected by Auger Electron Spectroscopy, and the density of visible impurities in the STM images was typically below $1/\mu m^2$. High-purity borazine, $(HBNH)_3$, was gratefully obtained from the group of Prof. Hermann Sachdev at the University of Saarland in Germany and was deposited in the UHV-system from a dosing nozzle, that stored the material at a reduced temperature, by means of a Peltier cooler, and allowed it to warm up for deposition purposes. The cooling/dosing system was thankfully received from Prof. Jürg Osterwalder and Prof. Thomas Greber from the University of Zurich in Switzerland.

Most of the measurements in this part consist of in-situ STM imaging, namely at elevated temperatures and during deposition. By this method, one can achieve direct observations, which are far easier for understanding the mechanisms than images or other measurements carried out after completion of the growth procedure. However, the

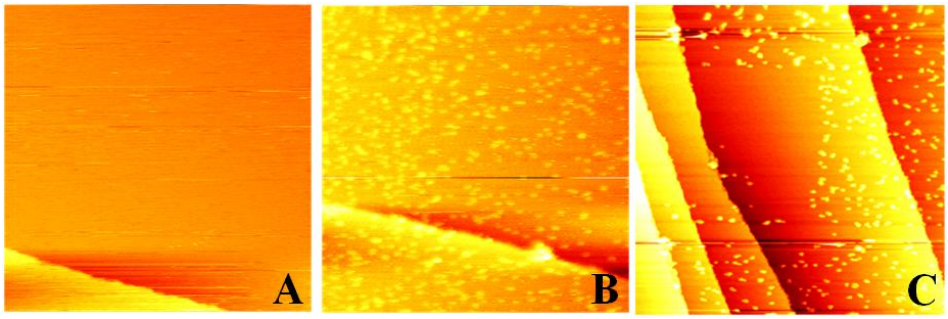

Fig. 3.1 Examples of the influence of the tip on the borazine deposition: (A) A Rh surface being scanned by STM, during borazine deposition. No deposits are visible on the surface. The feature at the bottom of the image is a monoatomic step on the Rh substrate. (B) An equally large region directly on the left-hand side of area that was scanned during deposition (image A). After deposition, many adsorbed borazine molecules are visible in this image. Notice the gradient in density from right (where the tip had been) to left. (C) A zoomed out STM image, after the central part had been imaged by the STM after the Rh surface had been dosed with 0.2 L of borazine at room temperature and annealed to 576 K. Small clusters had been formed during the annealing. The image shows that the clusters have been removed from the central region by the STM tip. The imaging conditions for the central region of panel C had been the same as the imaging conditions for the zoomed-out scan of panel C itself.
The image sizes of panels A and B are 85 × 85 nm^2, while that of panel C is 200 x 200 nm^2. Sample voltage: V_b = 2.5 V, 2.0 V, and 1.7 V, for fig. A, B, and C, respectively. Tunneling current I_t = 0.05 nA.

presence of the STM tip may influence the deposition. In particular, it can shadow off the portion of the surface that is being imaged, thus making the local deposition rate lower than the average rate. In the present work, it was found that the STM tip sometimes completely blocked the deposition of borazine molecules. For example, in Fig. 3.1, after 0.2 L (1 Langmuir = 10^{-6} torr s) of borazine exposure, the area that was scanned by the STM was still completely clean (panel A), while the direct surroundings had very noticeable amounts of borazine adsorbed (panel B). In addition to being an obstacle for the impinging molecules, the tip can also act as a 'vacuum cleaner', emptying the scanned area, even when it is covered already by adsorbed borazine molecules or clusters. Such effects may be particularly strong at elevated temperatures. An example of this tip-induced 'cleaning' can be found in Fig. 3.1C. Occasionally the tip switched spontaneously from the 'cleaning' configuration to normal behavior, in which it did not influence the surface, suggesting that the 'cleaning' did not depend on sample voltage or

tunneling current but on the configuration details of the tip. A possible explanation for this is that the 'cleaning' results from the interaction (Van der Waals or electrostatic) of the full tip with the borazine. If the structure of the very apex of the tip changes in such a way that it protrudes less far from the body of the tip, this interaction is significantly increased, thus possibly switching on the 'cleaning' effect, seemingly without significant changes in imaging quality.

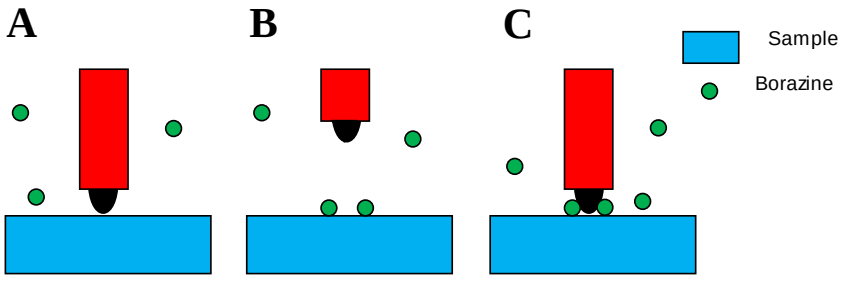

Fig. 3.2 Sketch of the tip retraction procedure. During STM imaging, borazine molecules sometimes cannot reach the scanned area because of geometrical blocking by the STM tip (A). In such cases we adopted the procedure to retract the tip during one entire image period (B), so that borazine could reach the sample surface. After this the tip was returned to the measurement position, to acquire a single STM image. This (B)/(C) procedure was repeated throughout the entire deposition.

The blocking of the borazine deposition made it very difficult to perform STM measurements during deposition. Fig. 3.2 shows our method to circumvent this problem when it presented itself. The STM tip was retracted between subsequent STM frames for the duration of an entire STM frame. This meant that there was an empty image between every two scanned images. During the empty imaging, the borazine could reach the scanned area and react, so that this procedure effectively reduced the borazine exposure by a factor 0.5 (or slightly above 0.5) with respect to completely unhindered exposure. One disadvantage of our retraction procedure is the significant creeping of the piezo-electric scanner that follows after each substantial change in position. Even though the retraction (and re-approach) were directed along the z-direction, perpendicular to the surface, also the x- and y-position was found to exhibit a strong creeping effect that lasted for typically 30 minutes after the last re-approach. This creeping made it difficult to

relocate the original area that had been in view before a retraction–re-approach cycle. In addition, in the slow scan direction the creeping resulted in a nonlinear elongation of the image, which introduced the risk of large errors in the counting of the areas of islands or vacancies. Fortunately, the growth of the nanomesh structure was observed to follow a very specific mode, in which the growth unit was precisely equal to one complete unit of the nanomesh pattern, corresponding to 169 units of the BN overlayer. Usually the area of the growing *h*-BN could be identified just by counting the additional nanomesh units.

3.3 This part of the thesis

In this part of the thesis, we concentrate on the assembly of *h*-BN nanomesh films on Rh(111) by *in-situ* STM observations under the reported growth conditions, i.e. *during* borazine deposition, at temperatures up to 1200 K. Experimental procedures are provided in section 3.2. In the same section it will also be pointed out that the STM tip can block the borazine molecules from landing on the surface of the sample. A method will be introduced for avoiding such a tip influence. In Chapter 4, the behavior of *h*-BN and borazine at different temperatures will be investigated by deposition of borazine at various temperatures. The growth unit is found to be one entire unit cell of the nanomesh pattern. We will also consider the different edges (boron terminated and nitrogen terminated) of the nanomesh islands and we will discuss the energy barriers for growth on different sites in section 4.4.4. In Chapter 5, the adsorption of borazine and the temperature needed for its decomposition will be discussed. Chapter 6 will concentrate on the formation and stability of defects in the *h*-BN nanomesh. Based on this, we can understand why a high deposition temperature is needed for a high-quality nanomesh structure and an optimal growth recipe will be derived.